International Journal of Microwave and Wireless Technologies, 2010, 2(3-4), 359–367.
doi:10.1017/S1759078710000358

De-ghosting of tomographic images in a radar network with sparse angular sampling

ANGIE FASOULA[1], HANS DRIESSEN[2] AND PIET VAN GENDEREN[3]

Taking into account sparsity of the reflectivity function of several radar targets of interest, efficient low-complexity automatic target recognition (ATR) systems can be designed. Such ATR systems would be based on two-dimensional (2D) spatial target models of low dimensionality, where critical information on the radar target signature is summarized. Discrete 2D radar target models can be estimated using high range resolution (HRR) data, measured at a sparse system of view angles. This being the main objective, incoherent tomographic processing of HRR data from a distributed surveillance system, made up of several radar nodes, is studied in this paper. A sparse angular sampling scheme is proposed, which exploits diversity due to both the distributed radar system and the target motion. The novelty is in the exploitation of this locally dense, but otherwise sparse set of viewing angles of the targets, obtained using a sparse network of radars. The de-ghosting efficiency of such a sampling scheme is demonstrated geometrically. This results in identification of minimal information resources for unambiguous estimation of a 2D target model, useful for radar target classification.

Keywords: 2D radar imaging, Radar network, High resolution, Incoherent back-projection, Sparse sampling, De-ghosting

Received 21 December 2009; Revised 26 February 2010

I. INTRODUCTION: INCOHERENT PROCESSING IN DISTRIBUTED RADAR SYSTEMS

An important property of a radar network is the angular diversity of the overall acquired information. In the specific case of an high range resolution (HRR) radar network, multi-aspect HRR profiles of the same radar target are collected. The available data in such a system are one-dimensional (1D) projections of the two-dimensional (2D) target reflectivity function at few, widely separated, view angles. In this scope, the question of interest is whether a low-dimensional 2D target model can be unambiguously estimated, using the HRR profiles that are measured at a sparse scheme of view angles. This sparse angular sampling scheme results from the multiple radar nodes at multiple moments in time, while the target is moving.

The 2D spatial target model to be estimated is defined in a feature space of low dimensionality. The dimensions of the feature-space correspond to features that are associated to the most important, in terms of scattered power, bright spots of the extended radar target. At a first approach to the problem, the considered features will only include the 2D position and the intensity of a small number of bright spots. An increased dimensionality of the feature space, by attaching more features to each bright spot, or by increasing the number of bright spots, would lead to a more informative description of the target structure. On the other hand, keeping the dimensionality as low as possible leads to simpler radar target classifiers, easier manageable databases, and smaller required measured datasets. The decision of the most appropriate dimension for the feature space is a trade-off between complexity and amount of retained information and clearly depends on the application.

While working with wide angular coverage, provided by the distributed radar system, tomographic image reconstruction techniques can be used. Based on the projection-slice theorem, the tomographic reconstruction generates an image, by individually back-projecting each HRR profile on a 2D grid of image pixels [1]. This formulation allows incoherent joint processing of data from multiple monostatic coherent radars in a distributed radar system. As in computerized tomography applications, only the amplitudes of the multi-aspect projections can be used to form the 2D image. In comparison with the coherent methods Synthetic Aperture Radar (SAR modes), the incoherent tomographic reconstruction achieves the same quality of image resolution, while operating with much wider angular coverage [2, 3].

The reconstructed 2D image is intended to be used as input for a parametric estimation algorithm. The final output will be an estimation of a target model in 2D space, consisting of the locations and the intensities of the most important bright spots of the target [4]. This model would offer significant benefits in automatic target recognition (ATR) systems and would support target classification.

Thinking of the 2D rigid-body target model as a sparse function in 2D space [5], a sparse angular sampling scheme is expected to be sufficient for unambiguous retrieval of the 2D target model [6, 7]. The herein presented study is focused on angular sampling principles for efficient de-ghosting and unambiguous 2D target model extraction, from 2D images which are generated with back-projection of a small set of HRR profiles.

It should be clarified though, that this work does not have the unrealistic objective of perfect unambiguous 2D imaging of the object with a limited, highly sparse dataset. The objective is rather to define the mechanisms for progressive alleviation of the ambiguities. Only the part of the 2D image that exceeds a meaningful intensity threshold will, at a further step, feed the

[1]Thales Nederland BV, Delft, The Netherlands.
[2]Thales Nederland BV, Hengelo, The Netherlands.
[3]IRCTR, Delft University of Technology, Delft, The Netherlands.
Corresponding author:
A. Fasoula
Email: angie.fasoula@thalesgroup.com

parametric estimation algorithm, which will be responsible for extraction of the 2D low-dimensional target model. What isof importance in this context is to assure convergence to an unambiguous estimation and further specify the expected rate of convergence, given the available resources.

The rest of the paper is structured as follows: in Section II, a geometrical interpretation is presented for the two main angular sampling principles for de-ghosting, when incoherent sparse sampling is used. In Section III, the sampling principles for the incoherent method are parallelized with the ones for coherent processing of multi-perspective radar data in an ISAR mode. In Section IV, a sparse angular sampling scheme with de-ghosting efficiency is presented. This is generated by a network of HRR radars at consecutive scans, while an extended radar target is moving. In Section V, a simulation example is given, where the proposed sparse angular sampling scheme is applied to 2D imaging of an extended object with sparse 2D reflectivity profile. The paper is closed with conclusions and discussion in the last Section VI.

II. SAMPLING PRINCIPLES: A GEOMETRICAL INTERPRETATION

A) Wide-angle sampling for resolution enhancement

As indicated in Fig. 1(a), two radars of range resolution ΔR which receive a radar target echo at two different view angles, with angular separation $\Delta\theta$, achieve in combination with each other a cross-range resolution ΔR_{eff}, which is equal to

$$\Delta R_{eff} = \frac{\Delta R}{\sin \Delta\theta}. \quad (1)$$

The ellipses in the figure represent the radar resolution cell. The short axis of each ellipse is equal to the range resolution ΔR, whereas the long axis is equal to the single-radar cross-range resolution, as defined by the antenna beamwidth and the range at which the target is seen.

It is intuitively expected, but also clearly visualized in Fig. 1(b), that by widening the angular separation $\Delta\theta$ between the contributing radar views, thinner resolution of the objects is achieved in 2D space. Resolution ΔR at both dimensions x and y is ultimately achieved, by combining two orthogonal radar views ($\Delta\theta = 90^\circ$).

The example images shown in Fig. 1(b) have been generated by incoherently back-projecting HRR data from two radars with $\Delta R = 0.5$ m and view angles instantaneously separated by $\Delta\theta = 30$, 60 and 90° correspondingly. Two reflectors are present at positions: $(x_1, y_1) = (2, 7)$ m and $(x_2, y_2) = (8, 3)$ m in the imaged radar scene. As highlighted by this simple example, the side effect of rapidly increasing the 2D local resolution with highly sparse multi-radar data, is the creation of ambiguities: the so-called ghosts. It is further explained in the following paragraph that these ambiguities can be removed by jointly using closely separated angular samples, acquirable at consecutive radar scans due to displacement of the object between the successive angular samples.

B) Thin-angle sampling for de-ghosting

With reference to Fig. 2, an area of interest LXL is considered for target imaging, where L is in the order of the target size. A very simple extended object, which consists of two-point scatterers is assumed. The two scatterers are separated by Δx and Δy at the two spatial dimensions which correspond to the line-of-sight direction of the two radars at time step t_1. The two radar views have an angular separation $\Delta\theta = 90^\circ$ at t_1. The $\Delta\theta$ being wide enough, the two scatterers are separated with high resolution at both dimensions, but two ghosts of equal strength are created at symmetrical positions.

Let us consider now the composite image, where HRR data from a following scan t_2 of one of the radars have been back-

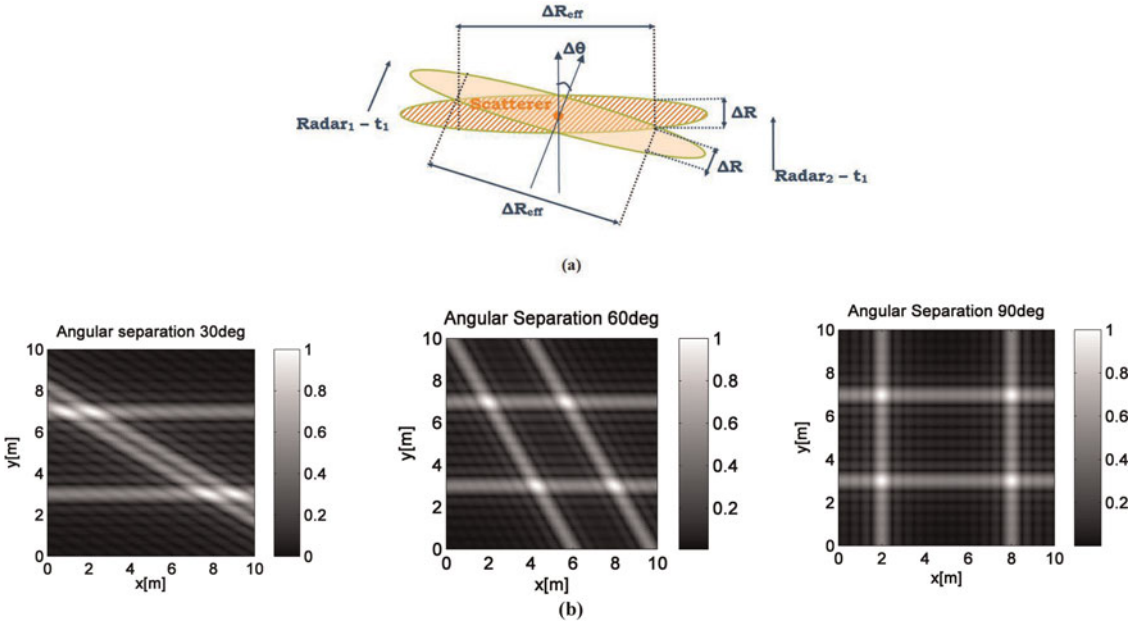

Fig. 1. (a) Cross-range resolution achieved with combination of two radar views with angular separation $\Delta\theta$. (b) Example: normalized 2D image (linear scale) of an extended object with two bright spots, using two radar views with $\Delta\theta = 30$, 60 and 90°.

https://doi.org/10.1017/S1759078710000358 Published online by Cambridge University Press

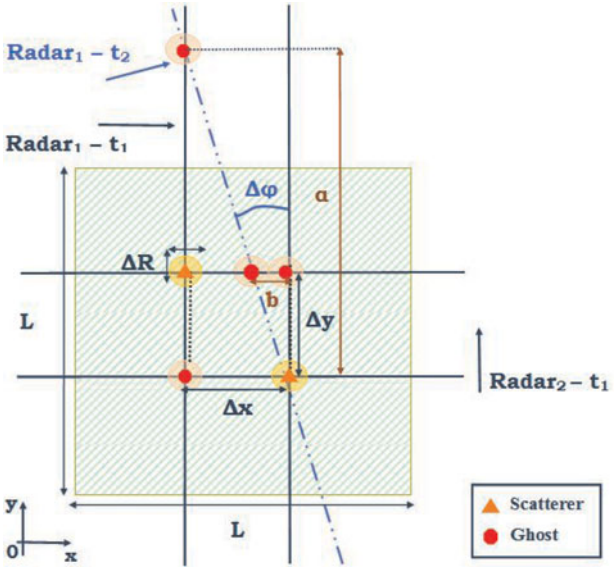

Fig. 2. Alleviate ghosts with use of multi-scan radar data.

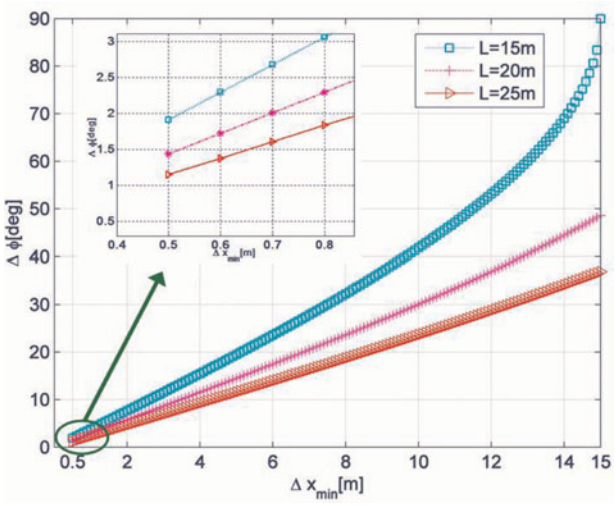

Fig. 3. Avoid creation of new ghosts with use of multi-scan radar data.

projected. The strength of the ghosts would appear degraded in the new image, if the target view angle by the radar was modifiedby $\Delta\phi$ when the new contributing data were collected. Two main constraints, which define the angular sampling $\Delta\phi$ useful for de-ghosting, are:

Constraint 1: Lower bound for angular coverage, to alleviate existing ghosts.

Compliance with this constraint intends to alleviate existing ghosts, by sharing their intensity with neighbor image pixels. According to the considered geometry of Fig. 2, this can be mathematically formulated as

$$b \geq \Delta R \Rightarrow |\Delta\phi| \geq \arcsin\left(\frac{\Delta R}{\Delta y}\right). \tag{2}$$

This constraint results in definition of a lower bound of angular coverage $\Delta\phi$, which is required to achieve de-ghosting in the 2D target image. The lower bound is scenario dependent. It is defined by the operational radar range resolution ΔR and the minimum separation Δy_{min} between the bright spots of the imaged extended object.

Constraint 2: Upper bound for angular sampling step, to avoid creation of new ghosts.

This constraint defines an upper bound for the angular sampling step $\Delta\phi$, such that creation of new ghosts is avoided within the imaging area of interest, with contribution of multi-scan data of each radar.

With reference to the geometry of Fig. 2, and while considering the worst case of a scatterer at the border of the imaging area *LXL*, this constraint can be mathematically expressed as

$$\alpha \geq L \Rightarrow |\Delta\phi| \leq \arcsin\left(\frac{\Delta x}{L}\right). \tag{3}$$

The upper sampling bound is plotted in Fig. 3 for various sizes L of the extended object and for various values of Δx_{min}, when the range resolution is $\Delta R = 0.5$ m. It is observable that the bound becomes more stringent as the complexity of the object increases. The complexity can be conceived as the number of bright spots, being jointly defined by Δx_{min} and the total size of the object L.

As indicated in the included zoom graph in Fig. 3, the case of object with the lowest possible sparsity factor, i.e. $\Delta x_{min} = \Delta R$, defines the critical angular sampling for unambiguous imaging in area *LXL*.

$$\Delta\phi_{critical} = \arcsin\left(\frac{\Delta R}{L}\right) \cong \frac{\Delta R}{L}. \tag{4}$$

III. PARALLELISM WITH SAMPLING PRINCIPLES FOR COHERENT PROCESSING OF MULTI-PERSPECTIVE RADAR DATA

It is interesting to compare the sampling principles which are given in equations (1) and (4) above, with the ones for coherent processing of multi-perspective radar data, in an inverse synthetic aperture radar (ISAR) mode.

In the case of coherent processing, the angular coverage $\Delta\theta$ which is required in order to achieve cross-range resolution ΔR_{eff} is defined as [8]

$$\Delta R_{eff} = \frac{\lambda}{4\sin(\Delta\theta/2)} \cong \frac{\lambda}{2\Delta\theta}. \tag{5}$$

The critical angular sampling $\Delta\phi_{critical}$ which guarantees unambiguous 2D imaging of an object of size L is given as [8]

$$\Delta\phi_{critical} = 2\arcsin\left(\frac{\lambda}{4\cdot L}\right) \cong \frac{\lambda}{2L}. \tag{6}$$

By comparison of the pairs: Equations (1) and (5), (4) and (6) it can be observed that in the incoherent approach the range resolution ΔR plays a role equivalent to the one of the half-wavelength $\lambda/2$ in the coherent approach.

https://doi.org/10.1017/S1759078710000358 Published online by Cambridge University Press

This means that one can think of the inverse of the fractional bandwidth as a scaling factor:

$$sc = \frac{\Delta R}{\lambda/2} = \frac{f_c}{B}$$

for the angular information resources, which are required by the two methods. The applicability of the proposed incoherent method when working with distributed radar systems, with wide angular coverage, is demonstrated this way.

IV. SPARSE ANGULAR SAMPLING SCHEME

In this section, the physics that are exploited in the studied system for unambiguous 2D target model retrieval are explained. A sparse angular sampling scheme with de-ghosting efficiency is formed using (A) radar echoes of a moving target at multiple scans, and (B) a distributed radar system.

A) Radar echoes of a moving target at multiple scans

Departing from the assumption of sparsity of the target reflectivity function, the minimum distance between bright spots in both dimensions

$$\Delta x_{min}, \Delta y_{min} = \gamma \Delta R,\ \gamma > 1$$

is assumed.

With reference to the graph of Fig. 2 and the explanation of Section II(B), this assumption means that angular samples $\Delta\phi$ in the span:

$$\arcsin\left(\frac{\Delta R}{L}\right) \le \Delta\phi \le \arcsin\left(\frac{\Delta x_{min}}{L}\right) \qquad (7)$$

are purely useful for de-ghosting.

A system of $M = 2$ radars with initially orthogonal views ($\Delta\theta = 90^\circ$) is further considered. Both radars acquire useful closely spaced angular samples in consecutive scans, due to displacement of the moving target. The bandwidth is for both radars $B = 300$ MHz, resulting in a range resolution $\Delta R = 0.5$ m. The size of the extended target to be imaged is $L = 15$ m in both dimensions. The lower and upper bound for useful view angles $\Delta\phi$, as defined in Section II(B), are drawn in Fig. 4 for the studied case.

It can be observed that for a target geometry with sparsity coefficient $\gamma \ge 6$, corresponding to Δx_{min}, $\Delta y_{min} \ge 3$ m, the upper sampling bound for avoidance of new ghosts is above the lower angular coverage bound for resolution of all existing ghosts. In the limit case of $\Delta x_{min} = 6\Delta R = 3$ m, the two bounds meet at the value $\Delta\phi \cong 12^\circ$. This means that, in this case, multi-scan data that provide angular samples between $\Delta\phi_{critical} \cong 2^\circ$ and $\Delta\phi_{max} \cong 12^\circ$ would purely contribute to alleviation of all ghosts in the 2D target image.

Assuming that the angular sector $\Delta\phi$ is covered by both radars in $K = 6$ scans, what is shown in Fig. 5 is the maximum of the ghost envelope at various linear cuts of the 2D target image, with contribution of the K-scan data for the aforementioned radar parameters.

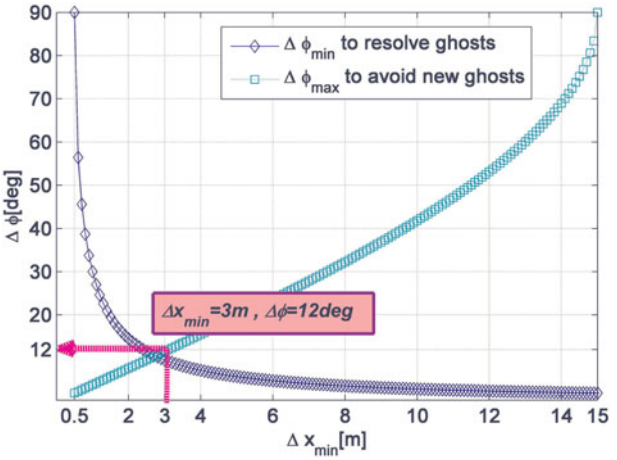

Fig. 4. Bounds of useful angular sampling.

Each linear cut is defined by a constant vertical distance Δy from one of the scatterers in the 2D image, which is taken here as a reference. The plot is given for various values of Δy and various values of the angular sector $\Delta\phi$, covered by both radars within $K = 6$ scans.

With reference to the geometry of Fig. 2, the maximum of the ghost envelope has been calculated as

$$I_{\Delta\phi,\Delta y} = max\left\{\sum_{t=0}^{K-1}\left|\mathrm{sinc}\left(\frac{2B}{c}(r - r_t)\right)\right|\right\} \qquad (8)$$

with

$$r_t = \Delta y \tan\left(t\frac{\Delta\phi}{K-1}\right), \qquad (9)$$

where $c = 3 \times 10^8$ m/s is the speed of light. The sinc is an appropriate descriptor of the waveform that we have been using [9]. Other waveforms may require a different model.

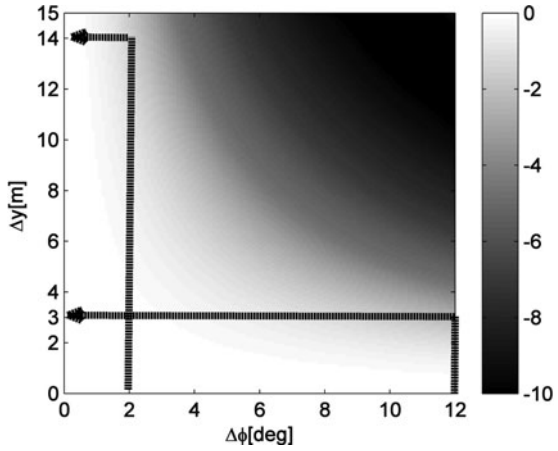

Fig. 5. Maximum of the ghost envelope (dB) at various linear cuts of the 2D target image and for various values of covered angular sector: normalized 2D visualization (two radars, six scans).

https://doi.org/10.1017/S1759078710000358 Published online by Cambridge University Press

It is observable that when $\Delta\phi = \Delta\phi_{critical}$, degradation of the ghost envelope starts at a distance $\Delta y \cong L$. When an angular sector $\Delta\phi = \Delta\phi_{max}$ has been covered, ghosts at distance $\Delta y \cong \Delta x_{min}$ are resolved by few dBs.

B) Distributed radar system

In Fig. 6, the beneficial effect of using data from $M > 2$ radars is visualized.

In this case the ghost envelope is re-calculated as

$$I_{\Delta\phi,\Delta y} = \max\{s_1 + s_2\},$$

$$s_1 = \sum_{t=0}^{K-1} \left| \mathrm{sinc}\left(\frac{2B}{c}(r - r_t) \right) \right|,$$

$$s_2 = \sum_{t=0}^{K-1} \sum_{m=3}^{M} \left| \mathrm{sinc}\left(\frac{2B}{c}(r - r_{m,t}) \right) \right|, \quad (10)$$

with

$$r_{m,t} = \Delta y \tan\left(\Delta\theta_m + t\frac{\Delta\phi}{K-1} \right), \quad (11)$$

r_t as defined in equation (9) and $\Delta\theta_m$ the angular separation between radar$_1$ and radar$_m$.

In Fig. 6(a) an overview of the maximum of the ghost envelope with data from $M = 3$ radars, at initial view angles 0, 90 and 30°, is given. In Fig. 6(b), the corresponding situation with data from $M = 4$ radars, at initial view angles 0, 90, 30 and 60° is depicted.

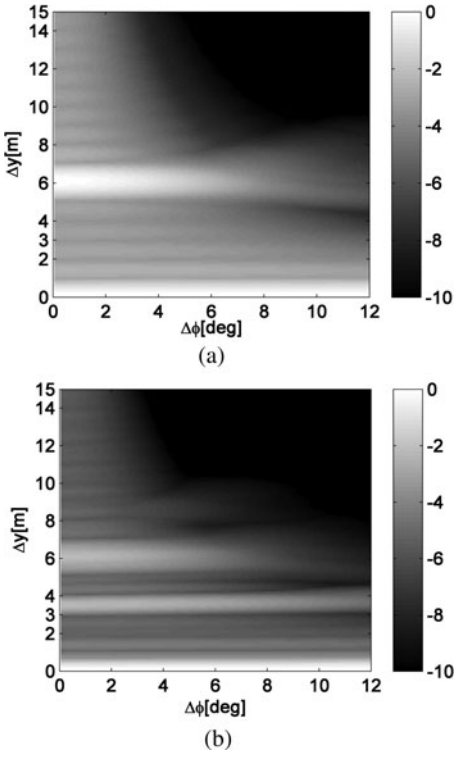

Fig. 6. Maximum of the ghost envelope (dB) at various linear cuts of the 2D target image and for various values of covered angular sector: normalized 2D visualization (a) three radars, six scans and (b) four radars, six scans.

The noticeable change in the system behavior is that ghosts at much smaller Δy_{min} are initially resolved by the contribution of a third or fourth radar. However the unavoidable side effect is that existing ghosts at positions (Δx, Δy) with respect to the reference scatterer may be strengthened as a consequence of the contribution of the mth radar, when $\Delta x = r_{m,t}$. This effect is target and system geometry dependent. One specific example is visualized in the above figures. The useful generalized remark that can be extracted through from this visualization is that strengthened ghosts get anyway alleviated at consecutive scans, resulting in overall accelerated de-ghosting performance of the multi-radar system.

V. SIMULATION EXAMPLE

The proposed sparse angular sampling scheme, supposedly originating from multi-radar multi-scan HRR radar measurements, has been applied for retrieval of the 2D target model of a specific target.

In the simulation application, this model is made-up of five-point scatterers of equal strength, which are positioned at

$$object = \begin{bmatrix} x \\ y \end{bmatrix} = \begin{bmatrix} 3 & 12 & 12 & 18 & 18 \\ 10 & 6 & 14 & 3 & 17 \end{bmatrix} \mathrm{m}$$

as depicted in Fig. 7.

HRR data of range resolution $\Delta R = 0.5$ m are collected from $M = 4$ radars, with initial view angles of the target: $\theta_1 = 0°$, $\theta_2 = 90°$, $\theta_3 = 30°$, and $\theta_4 = 60°$. All the four radars provide HRR data in $K = 6$ scans. The displacement of the moving target in each of the consecutive scans leads to angular difference in each radar view $\Delta\phi/(K-1) \cong 2.4°$, a bit higher than the critical angular sampling $\Delta\phi_{critical}$ for this scenario.

The images in Fig. 8 have been generated using back-projection of data from the two radars with initially orthogonal views. The left image shows the result after scan 1, whereas the right after scan 6. It is observed that closely spaced multi-scan data contribute to alleviation of existing ghosts, without creating new ones. However, the ambiguity area around the scatterers remains wide, compared to the resolution cell. These observations are in agreement with the analysis of Section IV(A). After six scans, an angular sector $\Delta\phi = 12°$ has been covered. This is the maximum $\Delta\phi$ that does not create new ghosts (ref. Constraint 2). The

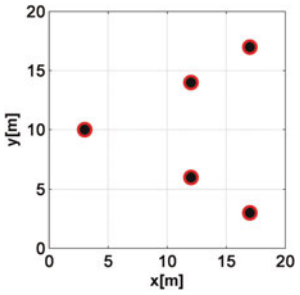

Fig. 7. 2D target model.

https://doi.org/10.1017/S1759078710000358 Published online by Cambridge University Press

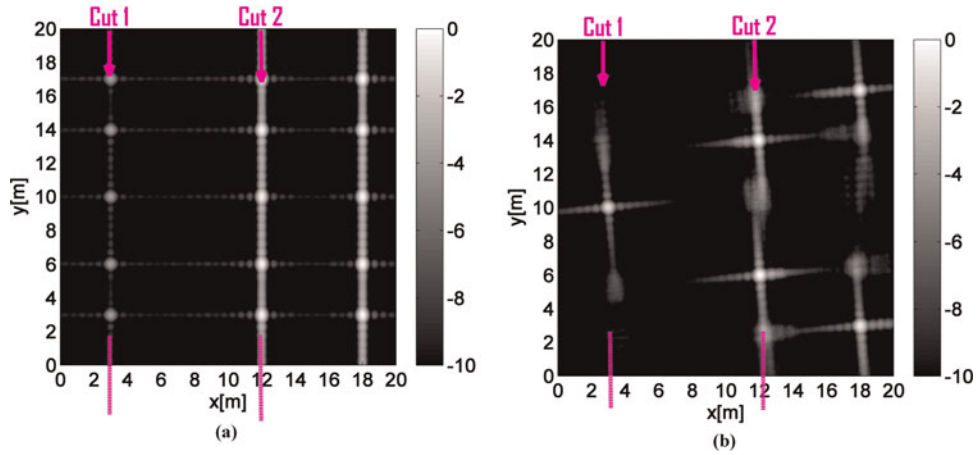

Fig. 8. Back-protection of HRR data from $M = 2$ radars at (a) scan 1 and (b) scan 6.

minimum Δx at which ghosts start to be resolved with such an angular coverage is $\Delta x_{min} = 3$ m.

In Fig. 9, the envelope of the 2D target image at two 1D linear cuts is visualized. Fig. 9(a) shows the linear cut 1: $x = 3$ m, where only one scatterer is present, the other four being ghosts. Fig. 9(b) shows the linear cut 2: $x = 12$ m, where two scatterers are present. In either graph, the linear cuts are given with differently coded lines for the 2D target image at consecutive scans of the two radars.

The objective of this visualization is to highlight the "windowing effect" of the multi-scan data. At consecutive scans, the widening of the covered angular sector $\Delta\phi$ due to target motion results in sharpening of the de-ghosting window and progressive alleviation of ghosts at closer vicinity to the real scatterers. Considering the threshold of -6 dB as decision limit for inclusion of the ghosts in the process of parametric estimation of the 2D target model, we can observe that the de-ghosting is accomplished only after six scans of the two radars at linear cut 1. At linear cut 2, the maximum considered number of six scans is not enough to drop the ghost envelope, below the desired threshold.

In Fig. 10 the improved 2D target images using data from all the four radars are shown for scan 1 in Fig. 10(a) and for scan 6 in Fig. 10(b). The use of widely separated multi-radar data retains the 2D resolution high, however existing ghosts are alleviated at the expense of the creation of new ones. In accordance with the analysis of the previous sections, the combination of multi-radar and multi-scan data results in the final right image. By exploiting the complementary effect of the two mechanisms,the image intensity gets accumulated around the true scatterers. With such a 2D image as input, unambiguous estimation of the 2D parametric target model is feasible [4].

In Fig. 11, the effect of an increased number of radars in the overall de-ghosting performance of the distributed radar system is isolated and illustrated. The same two linear cuts of the 2D target image, as in Fig. 9, are visualized here in the case that HRR data from only one scan but different number of radars are used. Ghosts are alleviated even at close vicinity to the reflectors, but some new ghosts are created at positions, that are dependent on the geometry of the extended object and the radar network.

The final Fig. 12 shows the multi-scan windowing effect, as applied to the data from $M = 4$ radars. Here the ghost envelope is degraded already at the first scan due to the multi-radar mechanism, but also includes some new ghosts, as suggested just before. The combined application of the multi-scan windowing effect leads to clearly improved de-ghosting performance of the distributed radar system. It can be observed that at linear cut 1 the de-ghosting process is accomplished already at scan 2 now. At linear cut 2, the desired degradation of the ghost envelope is achieved at scan 6 of the four radars.

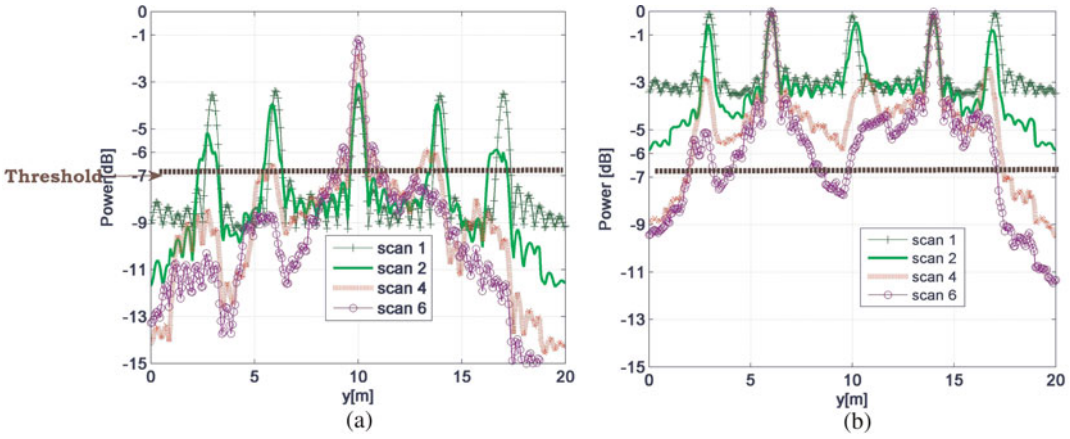

Fig. 9. (a) Linear cut 1 and (b) linear cut 2 of the 2D target image using data from two radars at multiple scans.

https://doi.org/10.1017/S1759078710000358 Published online by Cambridge University Press

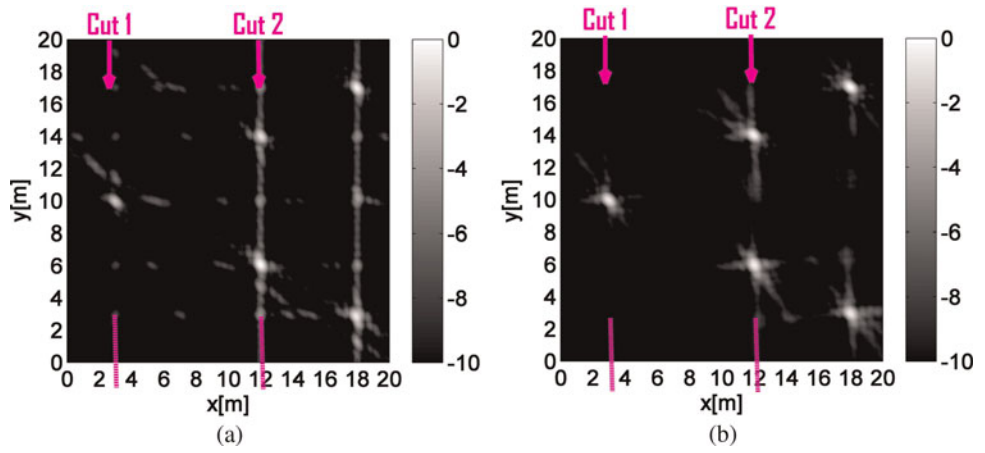

Fig. 10. Back-protection of HRR data from $M = 4$ radars at (a) scan 1 and (b) scan 6.

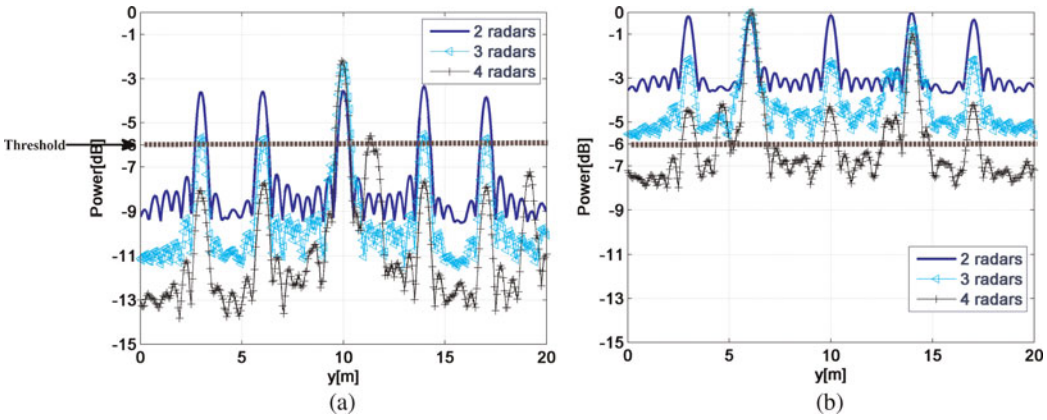

Fig. 11. (a) Linear cut 1 and (b) linear cut 2 of the 2D target image, using the first scan of multi-radar data.

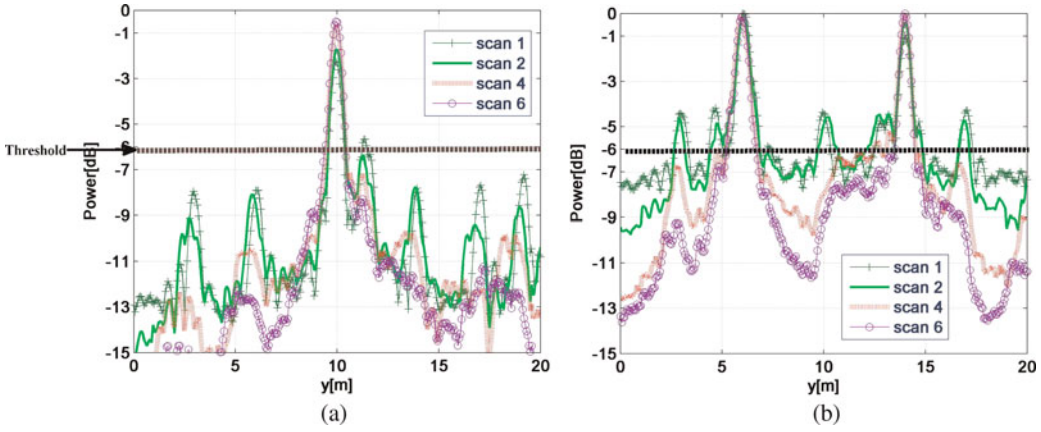

Fig. 12. (a) Linear cut 1 and (b) linear cut 2 of the 2D target image using data from four radars at multiple scans.

VI. CONCLUSIONS AND DISCUSSION

In this paper, guidelines for sparse angular sampling of the radar target reflectivity function have been proposed. Provided that this function is sparse in 2D space, unambiguous retrieval is achievable with a limited number of angular samples. It has been illustrated that the use of widely separated groups of closely separated angles is an efficient resource allocation scheme for achieving this. Such a scheme further fits to the scenario of a distributed surveillance system, observing a moving target.

In the proposed method, incoherent tomographic imaging is applied. A comparison with the sampling principles for coherent ISAR processing highlights the exchange of wide spatial coverage for accurate phase information.

https://doi.org/10.1017/S1759078710000358 Published online by Cambridge University Press

The method is designed for applications where radar targets with a sparse 2D RCS profile are involved. The presented 2D target images are meant as input for a parametric estimation algorithm. Unambiguous retrieval of a low-dimensional 2D model of the target, for use in ATR systems, is the actual objective. For a clear first demonstration of the principle, the simplest case of sparse 2D RCS profile, corresponding to a rigid-body radar target, has been considered in this paper.

In conditions that better resemble real life, the bright spots are expected to have a point spread function wider than the perfect spikes that were synthesized in the presented simulation application. By matching the high-value pixels of the 2D target image to a bivariate mixture model in the (x, y) 2D spatial domain, the estimation of the 2D target model can be robust to such effects though. The presented imaging approach is meant as pre-processing step for such a parametric estimation algorithm. For this reason, as already mentioned in the introduction, the topic of this paper is not the perfect unambiguous 2D imaging of the extended object. It is rather to define the sparse angular sampling principles that will assure convergence of the mixture model fitting process to an unambiguous solution.

In addition, partial visibility of the bright spots at widely separated view angles has to be taken into account in realistic scenarios. The partial visibility can result from both directivity of the individual bright spots and occlusion due to interaction between bright spots. Main associated complications that have to be considered then include: the possible need for a special fusion rule, other than simple averaging, of multi-radar widely separated radar views and the increased scatterer-to-ghost dynamic range for highly directive bright spots.

Finally, an interesting extension of this work is the coherent integration of the video per single-radar node in the network, resulting in local-only use of the phase in a distributed radar system [10, 11].The objective is an accelerated de-ghosting process by sharpening the multi-scan de-ghosting window, as a contribution of the phase history within the scan.

Results from application of the full method to radar measurements of real objects, where the above-mentioned complications have been observed, is also part of future work.

ACKNOWLEDGEMENTS

This project has received research funding from the Early Stage Training action in the context of the European Community's Sixth Framework Program. The paper reflects the authors' view and the European Community is not liable for any use that may be made of the information contained herein.

REFERENCES

[1] Griffiths, H.; Baker, C.: Fundamentals of tomography and radar, Advances in Sensing with Security Applications, Springer Netherlands, 2006.

[2] Desai, M.D.; Jenkins, W.K.: Convolution backprojection image reconstruction for spotlight mode synthetic aperture radar, IEEE Trans. Image Process., **1**(4) (1992), 505–517.

[3] Carrara, W.G.; Goodman, R.S.; Majewski, R.M.: Spotlight Synthetic Aperture Radar: Signal Processing Algorithms, Artech House, Boston, 1995.

[4] Fasoula, A.; Driessen, H.; van Genderen, P.: 2D parametric target model estimation using HRR data from a radar network, in Proc. Int. Radar Conf. 2009, Bordeaux, October 2009.

[5] Chevalier, F.L.: Principles of Radar and Sonar Signal Processing, Artech House, Boston, London, 2002.

[6] Baraniuk, R.; Steeghs, P.: Compressive radar imaging, in Proc. IEEE Radar Conf. 2007, Waltham, MA, 2007.

[7] Candes, E.; Romberg, J.; Tao, T.: Robust uncertainty principles: Exact signal reconstruction from highly incomplete frequency information, IEEE Trans. Inform. Theory, **52**(2) (2006), 489–509.

[8] Edde, B.: Radar Principles, Technology, Applications, Prentice Hall Inc., New Jersey, US, 1993.

[9] Tigrek, R.F.; Heij, W.; van Genderen, P.: Multi-carrier radar waveform schemes for range and doppler processing, In Proc. IEEE Radar Conf. 2009, Pasadena, May 2009.

[10] Moses, R.L.; Potter, L.C.; Cetin, M.: Wide-angle SAR imaging, In SPIE Defence and Security Symp., Algorithms for Synthetic Aperture Radar Imagery XI, April 2004.

[11] Stojanovic, I.; Cetin, M.; Karl, W.C.: Joint space aspect reconstruction of wide-angle SAR exploiting sparsity, In Zelnio, E.G.; Garber, F.D. (Eds.), SPIE Defence and Security Symp., Algorithms for Synthetic Aperture Radar Imagery XV, Orlando, FL, 2008.

Angie Fasoula was born in Trikala, Greece in 1982. She received the M.Sc. degree from the Electrical Engineering Department of the Aristotle University of Thessaloniki, Greece in 2005. From 2006 to 2009 she has been a Marie Curie research fellow in Thales Surface Radar, in Delft, The Netherlands. Now she is working as a radar system engineer in Thales Surface Radar in Limours, France. Since 2006, she is also a Ph.D. student in IRCTR (International Centre for Telecommunications and Radar) in TuDelft, the Netherlands. Her research interests include signal processing and data fusion in High Range Resolution (HRR) radar networks, for radar target recognition.

Hans Driessen received the M.Sc. and Ph.D. degrees in 1987 and 1992, respectively, both in Electrical Engineering from the Delft University of Technology. In 1993 he joined Thales Nederland B.V. (formerly known as Hollandse Signaalapparaten B.V.) as a design engineer of plot processing and target tracking systems. He is currently RD manager and technical authority in the area of radar system design and the associated sensor management, and signal and data processing. His professional interests are in the field of applied stochastic detection, estimation, and classification theory, with a focus on innovative radar applications of particle filtering and sensor management.

https://doi.org/10.1017/S1759078710000358 Published online by Cambridge University Press

Piet van Genderen received his Master of Science degree in Electrical Engineering from the University of Twente in Enschede, The Netherlands in 1971. His thesis was in information theory. After graduation, he joined the National Aerospace Laboratory in Amsterdam, The Netherlands until 1979. Since then he has been working with Hollandse Signaalapparaten BV in Hengelo, The Netherlands, now Thales Nederland. He held several positions in R&D as Group Expert Radar Systems. In 1994 he was appointed full professor at the International Research Centre for Telecommunications and Radar of the Delft University of Technology in The Netherlands. He has (co-)authored over 180 papers, seven patents and a few books. His current research interest is in radar management, adaptable waveforms, and false target recognition. Piet van Genderen is Member of the European Microwave Association. He has been awarded three times as author/co-author with the Radar Prize of the European Radar Conference (EuRAD), has received the prize for the most innovative and effective patent of the Thales group in 2000 and received an honorary doctorate of the Military Technical Academy of Romania. He has been the general chairman of the European Microwave Week in 2004 and the chairman of the European Microwave Conference during this event. He has been member of the technical program committee of many international conferences dedicated to radar.

https://doi.org/10.1017/S1759078710000358 Published online by Cambridge University Press